



ELSEVIER

Organic Electronics 2 (2001) 65–73

**Organic
Electronics**

www.elsevier.com/locate/orgel

High performance organic semiconducting thin films: Ink jet printed polythiophene [*rr*-P3HT]

Stuart P. Speakman^{a,b,c,*}, Gregor G. Rozenberg^{a,*}, Kim J. Clay^c,
William I. Milne^b, Adelina Ille^b, Ian A. Gardner^c, Eric Bresler^c,
Joachim H.G. Steinke^{a,*}

^a Department of Chemistry, Imperial College of Science, Technology and Medicine, South Kensington, London SW7 2AY, UK

^b Cambridge University Engineering Department, Trumpington Street, Cambridge CB2 1PZ, UK

^c Patterning Technologies Limited, Unit 7, The Maltings, Green Drift, Royston SG8 5DY, UK

Received 16 October 2000; received in revised form 18 December 2000; accepted 10 February 2001

Abstract

The piezoelectric ink jet (IJ) printing of an organic semiconducting ink, as applied to the fabrication of a thin film diode, has been demonstrated. IJ printed regioregular poly (3-hexylthiophene-2,5-diyl) [*rr*-P3HT] semiconducting films were directly patterned on to gold thin film contact surfaces. The resulting metal–semiconductor–metal diode exhibited low leakage current and a good forward–reverse current ratio. IJ printing of the P3HT as directly patterned thin films represents a significant step toward the realisation of cheap, large area, organic microelectronic devices and transistor active matrix backplanes. © 2001 Elsevier Science B.V. All rights reserved.

Keywords: Diode; Inkjet; Organic; Polymer; Polythiophene; Printing

Recent experiments have demonstrated that organic semiconducting and light emitting polymers can produce device structures with acceptable performance [1–3]. Indeed, commercial products such as light emitting polymer displays [4–6] and polymer transistor logic circuits [7] have been demonstrated. Integrated devices are now appearing [8–10], that make use of polymer transistor

switching, thus providing the potential for a cheap alternative to amorphous silicon thin film transistor (a-Si:TFT) technology [11,12]. Organic microelectronic device fabrication has made use of a wide variety of processing methods, including dip-coating, spin-casting, thermal evaporation, contact transfer (soft lithography), and screen printing [13–17]. In order to develop low cost, large area polymer electronic market opportunities (particularly device fabrication on flexible plastic substrates) solution-processable conjugated polymer development was primarily aimed at spin- and dip-cast processing. The need to combine large area coatings with device patterning, in order to accelerate progress in device manufacture, has fuelled

* Corresponding author. Tel.: +44-20-7594-5879; fax: +44-20-7594-5804.

E-mail addresses: stuart_PTL@btinternet.com (S.P. Speakman), g.rozenberg@ic.ac.uk (G.G. Rozenberg), j.steinke@ic.ac.uk (J.H.G. Steinke).

interest in developing direct-write fabrication methods. In this respect ink jet printing (IJP) is attracting much attention [18–21] as a potential manufacturing tool. Ink jet printing has a number of attributes that make a compelling argument for its evaluation and subsequent development for such a role. These include direct micropattern printing from a computer downloaded graphics file, very low material (ink) wastage, and high-speed parallel nozzle printing. The true promise of organic micro- and opto-electronics lies in the potential to produce all-polymer integrated circuits without the need to employ complex microlithography, in particular photolithographic patterning and other capital intensive processing as is the case with conventional amorphous and crystalline semiconductors and flat panel displays. Ink jet printing holds the promise of being a low cost manufacturing process, that will in the limit print all layers of such devices [22,23].

Early investigations [24,25] into ink jet printed device manufacture have shown that the process has considerable merit, but that work is required to realise stable ink formulations that are compatible with the available original equipment manufacturer (OEM) printhead designs and associated manufacturing materials, and which behave in a predictable and controllable fashion on selected substrate surfaces (e.g. indium–tin-oxide [ITO] coated materials, conducting polymers and contact metals). Although ink jet printhead droplet ejection can be achieved with thermal (bubble jet) and piezoelectric modes of pressure generation, the vast majority of the published literature on ink jet printing as a potential organic optoelectronic device manufacturing tool has been the result of using piezoelectric actuated printers [26,27]. Piezoelectric printhead technology is favoured primarily because it applies no thermal load to the organic inks and is compatible with the printing of digital images.

The present study describes, what is to the authors' knowledge, the first demonstration of a piezoelectric ink jet printed, directly patterned feature of an organic semiconducting ink containing polythiophene, that does not make use of a buffer layer to protect against process induced pinholes. The resulting thin film microstructure and

electrical behaviour has been investigated in a planar, vertically stacked, metal–semiconductor–metal (M–S–M) diode format and is reported here.

The ink jet printing set-up used in the present study was based on a custom-built PZT piezoelectric ceramic unimorph research printhead. This printhead design operates in the bend-mode (radial expansion of piezoelectric ceramic causes a bending moment in the bilaminar actuator [unimorph]), which provides the necessary pressure pulse capability to support drop-on-demand jetting behaviour from a range of nozzle diameters (25–300 μm). Both static (CCD camera droplet imaging with PC-based framegrabbing and image processing) and dynamic printing (CAD x – y image printing) facilities were available employing this printhead. The drop-on-demand printing was undertaken in a standard laboratory environment comprising an air ambient, non-particulate filtered enclosure (typically class 10,000), with no temperature or humidity control (although monitored as a control for data analysis). The object being to perform the printing under non-cleanroom conditions in order to determine the extent to which useable devices could be fabricated in a basic laboratory facility, thereby providing information on the necessary hardware modifications to be introduced on an industrial-scale printing system.

The organic semiconductor ink employed consisted of a commercially obtained regioregular poly (3-hexylthiophene-2,5-diyl) [*rr*-P3HT] dissolved in chloroform and chlorobenzene.¹ The solid content was limited to 0.7% w/w (chosen to facilitate a high solid content without promoting precipitation in the nozzle). The solution was sonicated in an ultrasonic bath, in order to minimise sedimentation and precipitation, and filtered before use. No other treatment was implemented for this initial study, although highly filtered solutions (using a 0.2 μm PTFE-filter) have been found by the authors to give optically smoother films with-

¹ This material was purchased from Aldrich Chemicals Co., Gillingham, UK. The average molecular weight (M_w) of this material is $\approx 87,000$.

out any signs of particulate inclusion [28]. It has been shown that *rr*-P3HT has a better than 98.5% head-to-tail linkage and its synthesis and properties have been previously described [29,30]. Due to the highly ordered, self-assembled, semi-crystalline structure of the formed polymer films, using the regioregular material, neutral and doping conductivities are higher than those measured for the regiorandom analogue [31]. As a result of its highly ordered structure the polymer also shows an increased propensity to form extended planar and therefore rod-like polymer chains, thus lowering its bandgap from 2.1 eV (regiorandom) to 1.7 eV (regioregular) [31], due to the extended conjugation length.

The substrate used in the diode fabrication was a 200 nm thick coating of gold (acting as a base contact for the M–S–M structure) thermally evaporated, as a whole area process, on to a 10 cm diameter silicon wafer. This wafer was then diced to provide individual test pieces. The diced substrates were cleaned using acetone, piranha acid² and finally washed with distilled water. Then they were dried in an oven for 2 h at 80°C and allowed to cool to room temperature prior to being presented in front of the research printhead using a nozzle plate-to-substrate spacing of between 0.5 and 2 cm. The top electrode of the M–S–M device was defined using a contact mask, through which a 200 nm thin film of gold or aluminium was thermally deposited. The basic *I–V* characteristics were recorded in air using a HP 4140B picoammeter-voltage source, but were shielded from ambient light and extraneous electrical signals within the all-metal enclosure that contained the device probing station. The custom probing station, employing pressure-sensitive stainless steel probes, was used to contact the device electrodes and the resulting data was acquired and processed using standard PC and data acquisition software.

Single solid dot features in the range 42–175 μm were analysed by scanning electron microscopy

(SEM). The observed features had cross-sections that were substrate dependent. Two basic cross-sections were observed, namely the conventional “Gaussian-like” and “thin solid centre, thick edge rim – doughnut-like” (see Fig. 1(a) and (b)).

The variable range of solid dots was investigated in order to determine potential size effects on the resulting film solidification process. Such size effects become potentially important when considering extrapolating the ink jet printing process from the current M–S–M diode fabrication to an electrode channel in-fill field-effect transistor

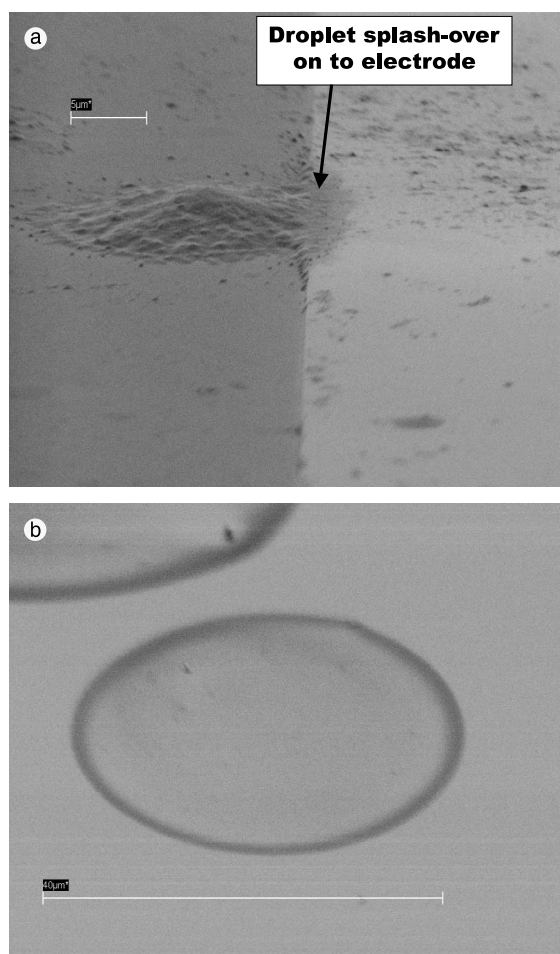


Fig. 1. SEM micrographs depicting (a) “Gaussian-like” and (b) “Doughnut-like” ink jet printed solid dots of *rr*-P3HT using both chloroform and chlorobenzene as the ink solvent.

² Piranha acid, which consists of a 1:1 mixture of aqueous hydrogen peroxide (30%) and concentrated sulphuric acid, is a highly corrosive solution that removes organic and inorganic matter efficiently.

(FET) build.³ Scanning electron microscopy was also employed to image the geometry and morphological quality (see Fig. 2(a) and (b)) of the resulting dots produced as a result of the ink jet printing of the *rr*-P3HT-chloroform and *rr*-P3HT-chlorobenzene inks from a range of nozzles.

Detailed examination of such dots clearly shows the existence of partially formed and collapsed bubbles within the thicker cross-section of the solid features. Very isolated early stage bubbles (blisters) were observed in the 50 nm thick coatings. The thin film formation behaviour and resulting properties of the annulus associated with the dot can be affected by changes to the ink formulation and the printhead droplet firing parameters, when modified with respect to a specified substrate material surface. However, both thinner (50 nm) smooth defect-free and thicker (approximately 1–2 μm) defective material exhibit similarly detailed solid state UV–VIS absorption spectra with clear peaks at 516, 552 and 608 nm, which is comparable to a drop-cast processed sample [32]. This suggests that a high level of molecular order is present in both types of coating, notwithstanding the occurrence of the defects observed.

It has been stated [33] that ink jet printing provides printed structures that after solidification contain defects such as pinholes. For poorly defined situations this can certainly be the case. In this context “poorly defined” means incompatibility between the selected ink properties (solid content, solvent type, viscosity, etc.) and the properties of the surface to be printed on, or the mechanics of the solidification process (i.e., rate of solvent evaporation) relative to the inertial dynamics of the liquid drop after impact. However, if attention is paid to the solid content of the ink and the droplet impact and wetting behaviour on the substrate surface of interest, it is possible to either

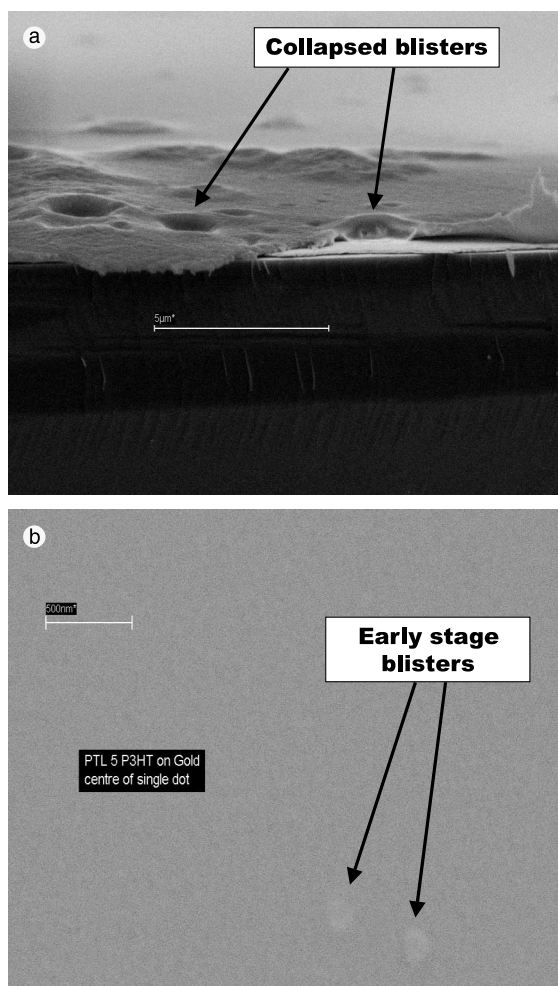


Fig. 2. SEM micrographs depicting (a) defective and (b) defect-free zones of ink jet printed solid dots of *rr*-P3HT.

control defect initiation and/or development to occur outside of the active area of the device (as observed in this study) or to eliminate such defects completely.⁴ By way of example, the printing set-

³ It is possible to build a P-FET (polymeric field-effect transistor based on an inverted-staggered structure) by depositing the organic semiconducting film before or after the drain-source electrodes have been deposited. The former promotes better metal contact interface reactivity. The latter promotes minimal interference of the semiconductor once printed, but requires good wetting between the semiconductor ink and the metal contacts in order to ensure an intimate coverage in the trench defined by the drain-source electrodes.

⁴ S.P. Speakman, G.G. Rozenberg and J.H.G. Steinke, Unpublished data relating to ink jet printing of organic semiconducting inks. For a MEH-PPV (1% w/w) tetrahydrofuran non-optimised ink formulation, drop impact mechanics promotes the on-set of a central drying zone that does not affect the basic coverage of the surface but does introduce a morphological transition between the impact and spreading zones. This is consistent with the computational fluid dynamic modelling [34].

up employed by Hebner et al. [19] using a polyvinylcarbazol (PVK)/dye/chloroform ink gave a solid dot profile [35]⁵ similar to that observed with the present study using a polythiophene–chloroform ink formulation. Hebner’s group observed a dot with a maximum in thickness at the centre of the dot, with a cross-section that approximates to a Gaussian and which has a high defect concentration (no image available but inferred from the comment in the paper that structure observed in optical micrograph attributed to solvent evaporation induced mass segregation). This was also observed by our group⁶ but only for large volume drops and occurred for both chloroform and chlorobenzene solvent-based inks. On both gold and aluminium thin film surfaces the ensuing ink jet printed solid dots were observed to have a drying edge that directly scaled with the dot diameter (due to drop volume). The edge width being 4% of the dot diameter, even when several dots were observed to have undergone coalescence, leading to the formation of a single drying edge. The observed edge is believed to be due to the competition between the surface wetting energy and the restoring force introduced by surface tension forces in the semi-liquid dot as the solvent is progressively liberated from the dot surface. The

⁵ It has not been possible to make a direct theoretical comparison between the two experimental projects because the details required for the mathematical model, relating to the use of the, we assume, Cannon PJ-1080A ink jet printer, and the liquid parameters of the PVK and dye-based inks, were not available from the publication cited here.

⁶ Data containing angle measurements [36].

Material	<i>rr</i> -P3HT	<i>rr</i> -P3HT	<i>rr</i> -P3HT	<i>rr</i> -P3HT	PANI-EB	PANI-CSA
Solvent	Chloroform	Chlorobenzene	p-xylene	toluene	NMP	m-cresol
Concentration	0.5% w/w	0.5% w/w	0.5% w/w	0.5% w/w	1% w/w	2% w/w
Substrate						
Copper	<5°	<5°	<5°	<5°	20°	20°
Gold thin film	<5°	<5°	<5°	<5°	5°	5°
Glass (microscope slide)	5°	5°	<5°	<5°	5°	20°
ITO thin film	5°	<5°	<5°	<5°	20°	20°
Polypropylene	5°	<5°	<5°	<5°	45°	45°
Polyethylene	10°	5°	5°	5°	20°	45°
PCB polymer mask	NA*	10°**	10°	10°	45°**	45°

* Dissolves and swells the substrate. ** The substrate swells if exposure to the solvent is prolonged.

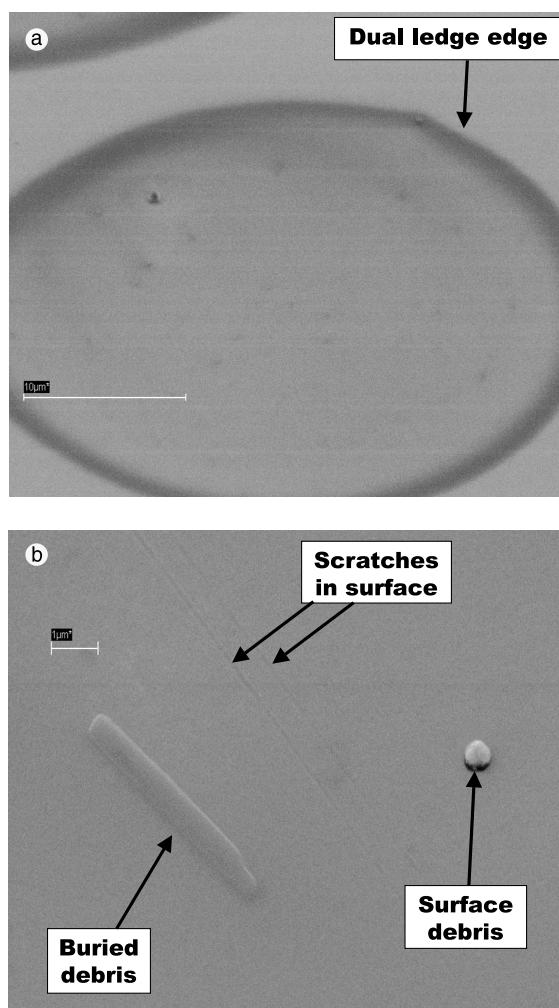


Fig. 3. SEM micrographs depicting (a) the quality and extent of the solidified dot drying edge and (b) the high magnification image of the film showing device quality ink jet printed *rr*-P3HT material.

drying edge is observed to be very thin and essentially defect free (see Fig. 3(b)) when imaged at a resolution of order 20 nm. The thickness and profile of the edge zone is believed to be substrate surface, jetting parameter, and ink property dependent.

Such solid dot geometry and defect differences relate to the properties of the jetted inks, the properties of the surface to be printed on, the inertial damping of the ejected droplet resulting from

the impact event and equilibrium phenomena, and the rate of solidification, which is influenced by the atmosphere of processing and the properties of the solvent(s) employed. For this study contact angles between the ink and a range of solid surfaces were measured that were used to predict the behaviour of the drop impact and solidification.⁶

Electrical characterisation of the IJP polythiophene was undertaken on a multilayer stack incorporating *rr*-P3HT. The multilayered structure being formed by the build-up of three sequentially printed lines, where the previously line was still semi-liquid at the time that the next layer was printed. The jet consisted of individual droplets, with an approximate 250 nm diameter, that were generated using a nozzle with 100 nm diameter exit hole. The droplet velocity was approximately 1 ms⁻¹ at a distance of 0.5 cm from the nozzle plane thus the impact velocity is estimated to have reached around 2.5 ms⁻¹ (close to being the terminal velocity). The SEM micrograph of the device cross-section (see Fig. 4(a)) shows no evidence of layer interfaces, implying good miscibility between successive printed layers as was required here.

The deposited device contact diameter was determined by SEM to be $576 \pm 3 \mu\text{m}$ and was shown to have covered processing induced defects (see device top contact image in Fig. 4(b)). The I - V curve (Fig. 5(a)) of a typical M-S-M diode structure (Fig. 5(b)) shows the typical Schottky behaviour associated with metal-semiconducting polymer-metal device structures.

The rectifying nature (Schottky barrier) due to the aluminium electrode and the ohmic nature due to the gold electrode can clearly be seen. Evaluation of the basic I - V characteristics show that the IJP thin film possesses a low leakage current [10^{-11} A] at low bias potentials [0.5–0.6 V], notwithstanding the presence of a low density of partially formed and collapsed blisters. The diode forward current on/off ratio was observed to be high, being >1600 for a 2 V bias potential. The structural arrangement of the M-S-M device coupled with the magnitude of the drive potential placed a moderate electric field across the semiconducting film. Electric fields in the range from 1×10^3 to 2×10^4 V cm⁻¹ were applied across the polythiophene

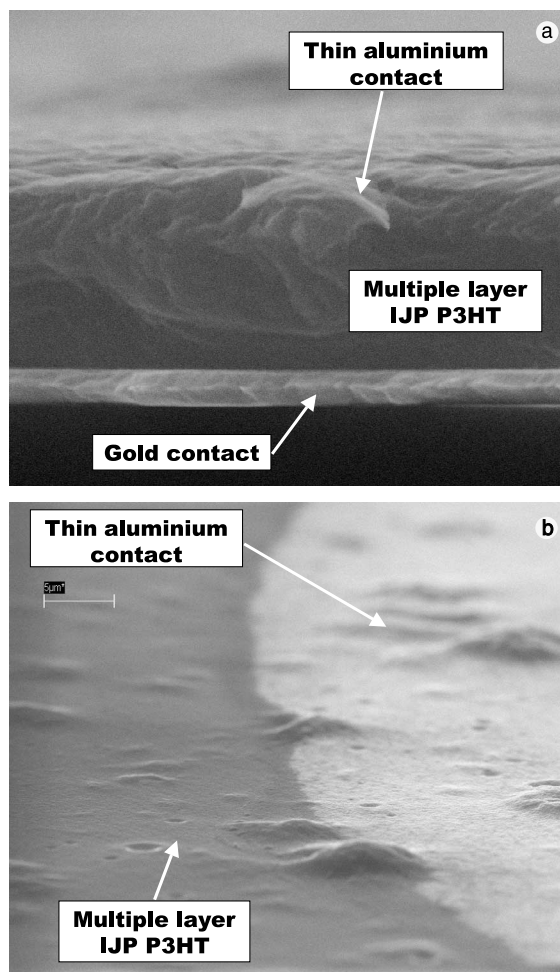


Fig. 4. SEM micrographs depicting (a) $M_{\text{Au}}-S_{rr\text{-P3HT}}-M_{\text{Al}}$ device cross-section and (b) diode aluminium top contact.

semiconductor film.⁷ At the highest electrical stress field, associated with a 1.9 V bias potential, the device was passing a forward-current density of 1 mA cm⁻². The series resistance of the polythiophene thin film diode, in the forward bias mode, was calculated to be 730 k Ω . Voltage cycling hysteresis was observed which has been attributed to a combination of manufacturing and

⁷ Calculated by using 1 μm as the film thickness. Data from SEM cross-section analysis indicates a film thickness of order of $1 \pm 0.01 \mu\text{m}$.

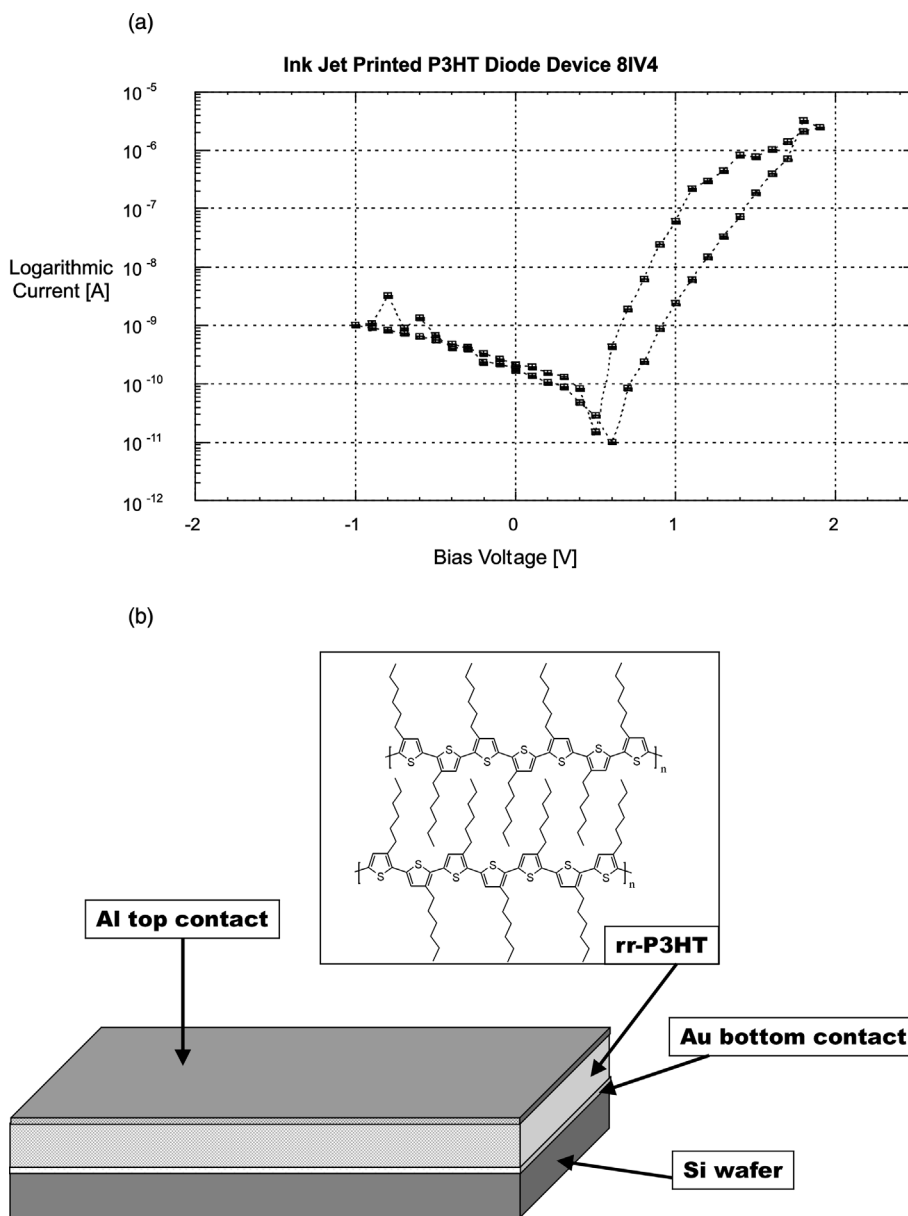


Fig. 5. (a) I - V characteristic for a M_{Au} - $S_{rr-P3HT}$ - M_{Al} vertically stacked diode structure and (b) a schematic of the M_{Au} - $S_{rr-P3HT}$ - M_{Al} diode structure showing the head-to-tail linkage of the rr -P3HT material.

analysing the device in air, resulting in interfacial oxidation and hydrogen-based mobile charge transport effects. The current does not saturate at large negative (reverse-bias) voltages, which it is believed is due to the presence of a contact-semiconductor interfacial layer.

The same device was investigated after being sealed in a polymeric membrane sample box for 3 months, no other precautions being taken. Initial exposure to a bias field, using the same set-up as described previously, showed a lower zero bias leakage current of approximately 2×10^{-13} A (at

the limit of meaningful data from the test equipment). The forward current slope possessed three activation stages (indicative of static and image force lowering effects) culminating in a permanent structural rearrangement that produced a higher operating current diode-like device. The I - V characteristic possessed no hysteresis and a forward current on-off ratio (at ± 1.4 V) of 27 was recorded. It is expected that oxygen and water vapour uptake has taken place, notwithstanding the nature of the sample box used to store the device. The defect nature of the film, as described above, is expected to promote fast diffusion pathways for the oxidising species to decorate/contaminate the P3HT film. This electric field induced structural rearrangement (electroforming) resulted in an increase in minimum current of approximately $10^6\times$, from 2×10^{-13} A to approximately 2×10^{-7} A. The observed increase in the zero bias leakage current after storage is ascribed to interfacial oxidation of the aluminium contact. The SEM analysis of the aluminium contact (see Fig. 4(b)) shows not only the film thickness (of order 30 nm) but also the presence of micro-perforations that would exacerbate interfacial contact oxidation. The *rr*-P3HT thin film M-S-M diode ideality factor has been determined to be high at a value of order 3.85 ± 0.32 based on the analysis of the conventional I - V characteristics. The data was well fitted over three decades and no account was taken for departure from ideal behaviour due to the presence of charge recombination effects. More detailed analysis is currently underway, but the initial non-optimised device data compares favourably with the literature values for polythiophene-based devices of order 2 [37], given the limits imposed on the manner in which the device was fabricated. The measured forward current onset voltage, V_0 , was 0.6 [-0.1, +0] V.

It has been shown that *rr*-P3HT films have a microcrystalline form that induces high charge mobility throughout the film [38]. The devices constructed in this study have not yet been X-ray analysed, so it is not possible to assign a solidification crystallisation orientation (in-plane or out-of-plane stacking relative to the electric field orientation as defined by the contact electrode configuration) and associated degree of alignment

and structural homogeneity. It is possible that pockets of microcrystallinity (polymer defects promoting interrupted conjugation) can exist for a film formed on an amorphous or polycrystalline surface, notwithstanding the self-assembly nature of the polymer. Self-ordering template polymers (two-dimensional, highly-ordered, single mono-layer films), based on silanes, are currently under consideration as a means of improving/homogenising head-to-tail coupling which enhances coplanarity between adjacent rings, thereby promoting greater π -overlap and consequent enhanced charge migration along the conjugated polymer chain.

In summary, the successful direct patterning of a polythiophene thin film using ink jet printing methods has been demonstrated. This represents an important step toward the realisation of cheap and reliable thin film organic microelectronic devices, particularly active matrix transistor switching backplanes. The IJP M-S-M polythiophene diode investigated in this study exhibited the following electrical properties:

- voltage cycling was observed to promote characteristic hysteresis producing a +0.26 V shift for a fixed output current of 1 nA,
- forward current onset voltage, $V_0 = 0.6$ [-0.1, +0] V,
- leakage current at V_0 is approximately 10^{-11} A (shortly after device preparation),
- forward bias exponential current turn-on occurs at 1 ± 0.1 V,
- forward current density at 1.9 V was 1 ± 0.01 mA cm⁻²,
- on-off rectification ratio at ± 1.9 V was 1625,
- forward bias series resistance was 730 k Ω at applied field of 1.9×10^4 V cm⁻¹.

We anticipate rapid progress in ink formulation and printing parameter optimisation leading to improved printed structure morphology and planarity. Such material and process optimisation will result in enhanced polythiophene diode and field-effect transistor behaviour comparable to, or better than, that observed for spin-cast or dip-cast processed material. We are actively pursuing the goal of an all-ink jet printed polymer integrated circuit and in this respect are pioneering the production of a generic manufacturing process.

Acknowledgements

One of the authors (SPS) would like to acknowledge the financial support resulting from the award of a Royal Society Industrial Fellowship.

References

- [1] A.R. Brown, C.P. Jarett, D.M. deLeeuw, M. Matters, *Synth. Met.* 88 (1997) 37.
- [2] Z. Bao, A. Dodabalapur, A.J. Lovinger, *Appl. Phys. Lett.* 69 (1996) 4108.
- [3] H. Sirringhaus, N. Tessler, R.H. Friend, *Science* 280 (1998) 1741.
- [4] World Wide Web sites of Philips (<http://www.philips.com>).
- [5] Uniax (<http://www.uniax.com>).
- [6] Cambridge Display Technology (<http://www.cdtltd.co.uk>).
- [7] Philips Research-Press Release Archive No. 97005e, 8 December 1997.
- [8] H. Sirringhaus, N. Tessler, R.H. Friend, *Science* 280 (1998) 1741.
- [9] C.J. Drury, C.M.J. Mutsaers, C.M. Hart, M. Matters, D.M. deLeeuw, *Appl. Phys. Lett.* 73 (1998) 108.
- [10] A. Dodabalapur et al., *Appl. Phys. Lett.* 73 (1998) 142.
- [11] Y.Y. Lin, D.J. Gundlach, S.F. Nelson, T.N. Jackson, *IEEE Electron Device Lett.* 18 (1997) 606.
- [12] H. Klauk, D.J. Gundlach, T.N. Jackson, *IEEE Electron Device Lett.* 20 (6) (1999) 289–291.
- [13] F. Garnier, R. Hajlaoui, A. Yassar, P. Srivastava, *Science* 265 (1994) 1684.
- [14] Z. Bao, Y. Feng, A. Dodabalapur, V.R. Raju, A.J. Lovinger, *Chem. Mater.* 9 (1997) 1299.
- [15] H.A. Biebuyck, N.B. Larson, E. Delamarche, B. Michel, *IBM J. Res. Develop. Optical Lithography* 41 (1/2) (1997) 1–11.
- [16] T. Granlund, T. Nyberg, L.S. Roman, O. Inganäs, Presentation Th-10, in: Second International Conference on Electroluminescence from Molecular Materials and Related Phenomena, Sheffield, UK, May 1999.
- [17] J. Feng, A.G. MacDiarmid, A.J. Epstein, *Synth. Metals* 84 (1997) 131–132.
- [18] K. Yoshimori, S. Naka, M. Shibata, H. Okada, H. Onnagawa, *Asia Display 98* 14.1 (1998) 213.
- [19] T.R. Hebner, C.C. Wu, D. Marcy, M.H. Lu, J.C. Sturm, *Appl. Phys. Lett.* 72 (1998) 519.
- [20] J. Bharathan, Y. Yang, *Appl. Phys. Lett.* 72 (1998) 2660.
- [21] H. Kobayashi, S. Kanbe, S. Seki, H. Kigchi, M. Kimura, I. Yudasaka, S. Miyashita, T. Shimoda, C.R. Towns, J.H. Burroughes, R.H. Friend, Presentation Th-7, in: Second International Conference on Electroluminescence from Molecular Materials and Related Phenomena, Sheffield, UK, May 1999.
- [22] S.P. Speakman, GB 9721808.5 patent application 14 October 1997, PCT/GB98/03087, 14 October 1998.
- [23] R.H. Friend, J. Burroughes, T. Shimoda, *Phys. World* 12 (6) (1999) 35–40.
- [24] E. Yamaguchi, K. Sakai, I. Nomura, T. Ono, M. Yamamoto, N. Abe, T. Hara, K. Hatanaka, Y. Osada, H. Yamamoto, T. Nakagiri, *SID 97 Digest* 6.2 (1997) 52.
- [25] K. Tamai, N. Ishimaru, Y. Hirai, T. Kamihori, *Asia Display 98* 13.3 (1998) 203.
- [26] L. Kuhn, A. Myers, *Scientific American* 240 (4) (1979) 162–178.
- [27] J. Heinzl, C.H. Hertz, *Adv. Electron. Electron Phys.* 65 (1985) 91.
- [28] G.G. Rozenberg, I. Gardner, J.H.G. Steinke, S.P. Speakman, unpublished data.
- [29] T.-A. Chen, X. Wu, R.D. Rieke, *J. Am. Chem. Soc.* 117 (1995) 233.
- [30] R.D. McCullough, S.P. Williams, *J. Am. Chem. Soc.* 115 (1993) 11608.
- [31] T.-A. Chen, X. Wu, R.D. Rieke, *J. Am. Chem. Soc.* 117 (1995) 233.
- [32] G.G. Rozenberg, I. Gardner, J.H.G. Steinke, S.P. Speakman, unpublished data.
- [33] Y. Yang, J. Bharathan, *Proc. SPIE-Int. Soc. Opt. Engng.* (1998) 3279, *Light-Emitting Diodes: Research, Manufacturing, and Applications II*, 78–86.
- [34] K. Yoshimori, S. Naka, M. Shibata, H. Okada, H. Onnagawa, *Asia Display 98* 14.1 (1998) 213.
- [35] T.R. Hebner, C.C. Wu, D. Marcy, M.H. Lu, J.C. Sturm, *Appl. Phys. Lett.* 72 (5) (1998) 519.
- [36] G.G. Rozenberg, S.P. Speakman, unpublished data.
- [37] H. Tomozawa, D. Braun, S. Philips, A.J. Heeger, *Synth. Metals* 22 (1987) 63.
- [38] H. Sirringhaus, P.J. Brown, R.H. Friend, M.M. Nielsen, K. Bechgaard, B.M.W. Langeveld-Voss, R.A.J. Janssen, E.W. Meijer, Presentation Fr-8, in: Second International Conference on Electroluminescence from Molecular Materials and Related Phenomena, Sheffield, UK, May 1999.